Elevated Visual Crowding in *CRB1*-Associated Retinopathies: Understanding Functional Visual Deficits Using Child-Friendly Computerized Testing

Ana Catalina Rodriguez-Martinez,[1,2,4] Vijay K. Tailor-Hamblin,[1–3,5] Bethany E. Higgins,[1–3,6] Pete R. Jones,[1–3,6] Tessa M. Dekker,[2,5] Robert H. Henderson,[1,4] John A. Greenwood,[5] and Mariya Moosajee[1–3,7]

[1]Moorfields Eye Hospital NHS Foundation Trust, London, England, United Kingdom
[2]Institute of Ophthalmology, University College London, London, England, United Kingdom
[3]NIHR Biomedical Research Centre at Moorfields Eye Hospital and UCL Institute of Ophthalmology, London, England, United Kingdom
[4]Great Ormond Street Hospital, London, England, United Kingdom
[5]Experimental Psychology, University College London, United Kingdom
[6]City St. George, University of London, London, United Kingdom
[7]The Francis Crick Institute, London, United Kingdom

Correspondence: Mariya Moosajee, UCL Institute of Ophthalmology, 11–43 Bath Street, London EC1V 9EL, UK;
m.moosajee@ucl.ac.uk.

ACRM and VKTH should be considered joint first authors. JAG and MM should be considered joint last authors.

Received: October 21, 2024
Accepted: April 2, 2025
Published: May 23, 2025

Citation: Rodriguez-Martinez AC, Tailor-Hamblin VK, Higgins BE, et al. Elevated visual crowding in *CRB1*-associated retinopathies: Understanding functional visual deficits using child-friendly computerized testing. *Invest Ophthalmol Vis Sci.* 2025;66(5):32. https://doi.org/10.1167/iovs.66.5.32

Purpose. Mutations affecting the *CRB1* gene produce retinal dystrophies including early onset severe retinal dystrophy/Leber congenital amaurosis (EOSRD/LCA), retinitis pigmentosa (RP), cone-rod dystrophy (CORD), and macular dystrophy (MD). As treatment strategies advance toward clinical translation, there is a need to establish reliable outcome metrics and to better understand the visual deficits associated with *CRB1* retinopathies. To this end, we measured visual acuity (VA) and crowding (the disruptive effect of clutter on object recognition), both key functions in spatial vision, using child-friendly computer-based tests, and gold-standard clinical measures.

Methods. Patients with molecularly confirmed biallelic *CRB1* pathogenic variants were compared with age-matched controls ($n = 20$ in each). Best-corrected visual acuity (BCVA) was measured with both Early Treatment Diabetic Retinopathy Study (ETDRS) and the computerized VacMan procedures (using an unflanked/isolated VacMan target), which also allowed measurement of crowding when surrounding flanker elements were added.

Results. Both acuity and crowding were significantly elevated in individuals with *CRB1* retinopathy compared with controls. ETDRS acuity correlated with both the unflanked ($r = 0.868$, $P < 0.001$) and flanked VacMan thresholds ($r = 0.748$, $P < 0.001$). No statistically significant changes in crowding were observed with respect to *CRB1* phenotype (EOSRD/LCA, CORD, or MD) or age of onset.

Conclusions. This study demonstrates for the first time that individuals with *CRB1* retinopathy exhibit elevated crowding in their foveal vision compared with controls. Measuring crowding offers valuable insights into understanding functional visual deficits in *CRB1* retinopathy and could be a useful metric for monitoring disease progression and treatment outcomes in inherited retinal diseases.

Keywords: *CRB1*, retinal dystrophy, inherited retinal disease, visual acuity (VA), visual crowding

CRB1 (*Crumbs homolog 1*) is a transmembrane protein essential for retinal development and long-term retinal integrity.[1] It regulates apical-basal polarity, outer limiting membrane (OLM) integrity, cell-cell adhesion, cellular signaling pathways, and maintains zonula adherence junctions at the OLM.[2,3] Biallelic pathogenic variants in the *CRB1* gene (OMIM #604210) have been identified to cause a broad spectrum of autosomal recessive retinopathies which cause different levels of visual impairment.[4] The most prevalent phenotype seen is severe is Leber congenital amaurosis (LCA8; OMIM #613935) with between 7% and 17% of reported cases having this presentation.[1] Other clinical presentations include early onset severe retinal dystrophy (EOSRD), often reported together with LCA as LCA/EOSRD, autosomal recessive retinitis pigmentosa (RP12; OMIM #600105), cone-rod dystrophy (CORD), and macular dystrophy (MD). Ocular features seen in *CRB1* retinopathies include nummular pigmentation, yellow punctate deposits, preserved para-arteriolar retinal pigment epithelium (PPRPE), coats vasculopathy, and a thickened

and coarse retina seen on spectral domain optical coherence tomography (SD-OCT).[1,4,5]

CRB1 retinopathies can affect various aspects of visual function, such as visual acuity(VA), color vision, contrast sensitivity, and peripheral vision, which can be monitored over time.[6] Although acuity assessed via the Early Treatment Diabetic Retinopathy Study (ETDRS) chart has been the primary outcome metric in both the routine clinical setting and in clinical trials,[7,8] ETDRS acuity does not provide a comprehensive characterization of visual function, and may fail to detect individual differences[9,10] or subtle changes in visual function.[6] Similarly, whereas the Pelli-Robson provides a quick overall summary measure of contrast sensitivity,[11] it does not quantify sensitivity at different spatial frequencies, requires the ability to read letters, and may not sustain interest in young children.[12] Other functional and structural tests, such as electro-diagnostic testing, microperimetry, and SD-OCT, have been explored.[13] However, regulatory bodies are still working to establish a functional endpoint that is meaningful for patients' visual function.[6,13–16]

To further explore functional endpoints, it is essential to first gain a comprehensive understanding of the visual deficits and then incorporate newly designed, child friendly tests to improve the accuracy of monitoring of disease progression in the pediatric populations. One measure of visual function that remains unexplored in inherited retinal diseases (IRDs), including *CRB1* retinopathies, is visual crowding: the disruptive effect whereby objects that are easily recognizable in isolation become difficult to identify when surrounded by other objects.[17] Crowding is a cortical process that places strong limits on peripheral vision in the typical adult visual system.[18] Disruptions are observed when flanker objects fall within an interference zone around a target.[19] In the typical periphery, the size of these interference zones increase with eccentricity such that the center-to-center separation of objects needs to be greater than half the target eccentricity to avoid crowding effects.[20,21] Crowding is typically minimal in the fovea,[20] but has been shown to be elevated in the foveal vision of typical children,[22,23] and even further in individuals with strabismic amblyopia,[24,25] and nystagmus.[26–28] Crowding has also been shown to be elevated in the peripheral field of individuals with glaucoma.[29–31] However, the effects of *CRB1* retinopathies on crowding are unknown.

Given the broad changes to the visual system caused by mutations in the *CRB1* gene, we hypothesized that visual crowding in patients with *CRB1* retinopathy will be elevated. These elevations may be noted especially in those affecting central vision, like LCA/EOSRD, MD, or CORD, although this is yet to be explored. Because typical children also show elevated levels of foveal crowding, we compared a molecularly confirmed *CRB1* cohort with age-matched controls. Clinically, VA charts incorporate contours, boxes, and neighboring optotypes to introduce "crowding" effects,[32] with varying levels of success.[30,33]

In the present study, we assessed crowding using the child-friendly VacMan task,[25] a modified Landolt-C recognition task, which uses four "ghosts" as flankers. This paradigm uses a modified staircase procedure to measure threshold size with both unflanked elements (to measure acuity) and in the presence of flankers (to measure crowding).[25,34] This study aims to examine these visual deficits using both the clinical ETDRS test and the child-friendly VacMan measures of both acuity and crowded acuity. The aim of the present study was to provide a better understanding of the visual deficits associated with *CRB1* and to evaluate potential outcome metrics of visual function for future use in clinical trials.

Methods

This was a prospective study at Moorfields Eye Hospital NHS Foundation Trust. Participants with biallelic (pathogenic or likely pathogenic) variants in the *CRB1* gene were identified from the Inherited Eye Disease database and invited to participate. Individuals were required to have a best-corrected visual acuity (BCVA) of 1.00 logarithm of the minimum angle of resolution (logMAR) or better in the better seeing eye. Patients and relatives gave written informed consent for genetic testing, through the Genetic Study of Inherited Eye Disease (REC reference 12/LO/0141). Age-matched control participants were recruited through local databases. All procedures adhered to the tenets of the Declaration of Helsinki.

Clinical Testing

Demographics, clinical data, medical and ophthalmic history, refractive error, fundoscopy, and ETDRS chart BCVA were collected from full ophthalmic assessments conducted at their visit. Patients were categorized into different phenotypes based on clinical data, retinal imaging, and age of onset, and grouped as EOSRD/LCA, MD, CORD, or RP. BCVA measurements were captured with the ETDRS ESV-3000 chart by Precision Vision using "letter-by-letter" scoring.

VacMan Apparatus

VacMan ran on a Dell PC (Dell, Round Rock, TX, USA), using MATLAB (The MathWorks, Ltd., Cambridge, UK) and PsychToolbox.[35,36] Stimuli were presented on a liquid crystal display monitor (SyncMaster 2233RZ LCD monitor; Samsung Electronics, Seoul, South Korea), with 1680 × 1050-pixel resolution and 120-hertz (Hz) refresh rate. To ensure that dark and light stimuli were equally balanced around the background grey, the monitor was calibrated with a photometer (Konica Minolta Sensing Americas, Ramsey, NJ, USA) and linearized in software, giving a maximum monitor luminance of 92.8 cd/m^2. The viewing distance was adjusted for each participant based on their BCVA measured on the ETDRS chart, with 3 meters (m) for those with <0.5 logMAR, 2 m for 0.5 to 0.7 logMAR, and 1 m for 0.7 to 1.00 logMAR. These distances ensured both adequate screen resolution to measure acuity levels and sufficient screen size to measure the extent of crowding. Participants wore their full refractive correction, including contact lenses, when necessary, with no additional correction for presbyopia. Verbal responses to the task (see below) were recorded by the experimenter using a computer keyboard. Testing was undertaken with both eyes open.

VacMan Stimuli and Procedure

The stimuli and procedures used to measure acuity and crowding were adapted from prior work.[25,34] These binocular tests involved a centrally located target known as VacMan – a "filled-in" Landolt C element presented at the screen's center (see Fig. 1A), with a "mouth" gap with a width one-

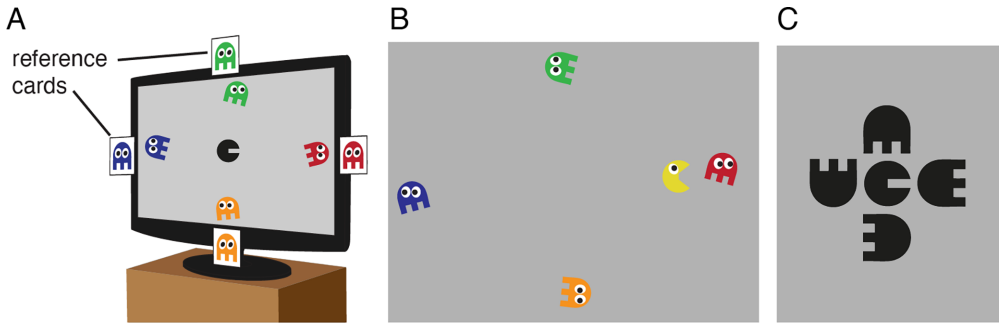

Figure 1. (**A**) An example trial of the unflanked VacMan task is depicted. Children reported the color of the ghost that VacMan was facing. Colored cards were present on the monitor edges for reference. (**B**) An example frame from the "reward animation." (**C**) Depiction of the crowding stimuli. Ghosts were rendered achromatically and presented at random orientations at a fixed separation from VacMan. The task was as in **A**, with the reference cards assisting color memory.

fifth the stimulus diameter, as with Sloan letters.[37] All participants began with the unflanked task, used to measure acuity. Here, VacMan was presented in the center of the display and rendered in black at 99% Weber contrast against a mid-grey background (see Fig. 1A). The four ghosts moved slowly along the monitor boundaries (approximately 2.2–4.48 degrees from the center), each with distinct colors (red to the right, green above, blue left, and orange below). On each trial, the target was oriented in one of four cardinal orientations, and participants were asked to identify the position of the "mouth" on VacMan (a 4-Alternative Forced Choice response). For younger children, the question was rephrased to "can you tell me which ghost VacMan wants to eat?" To aid responses to the psychophysical task, large reference pictures of the ghosts were attached to the monitor edges. This allowed children to report either the location of a ghost or, if preferred, its color. Responses were verbalized by the participant and the input was completed on a keypad by the examiner. Feedback was given after each trial, and "reward animations" (Fig. 1B) played after every three correct responses to maintain interest.

For the flanked task, used to measure crowding, the VacMan target was surrounded by four achromatic ghost flankers (Fig. 1C), with a center-to-center spacing between the target and flankers set at 1.1 times the size of the target, as recommended by prior work,[33] for both normal peripheral vision and foveal vision in amblyopia. On each trial, flankers were randomly allocated one of the cardinal orientations, without repeats. Participants once again reported the color of the ghost that the mouth of VacMan pointed toward, with the reference cards present as a reminder of these colors.

Stimulus sizes for both target and flanker elements (when present) were determined on each trial using a QUEST procedure – an adaptive psychometric procedure that uses responses to previous stimuli to set stimulus intensity on a given trial.[38] The staircase was set to converge on to 62.5% correct responses (at the midpoint of a psychometric function running from chance to 100% correct). As implemented previously,[28] we added variance to the gap sizes presented on each trial to avoid rapid convergence of the QUEST toward small stimulus sizes (which children can find frustrating). For the same reason, "catch" trials were presented four times in each task, with stimulus sizes set to triple to the current estimated threshold. These modifications also increased the reliability of the fitting of psychometric functions to the data,[39] which were fit across trials to determine the threshold for the unflanked and flanked conditions separately. Participants undertook five practice trials at the start of each block, which were not included in the analysis. Each block consisted of 40 trials, including the practice trials. Where possible, children completed two repeats of each condition (achieved in all but 2 of the children in the *CRB1* group). The whole experiment took 15 to 20 minutes.

As a follow-up, patients were surveyed to assess the enjoyability of the ETDRS and VacMan tests. Responses were collected using a 5-point scale with the following options: strongly enjoyed, enjoyed, neutral, disliked, or strongly disliked. Additionally, participants were asked to indicate their preference between the ETDRS test and the VacMan paradigm.

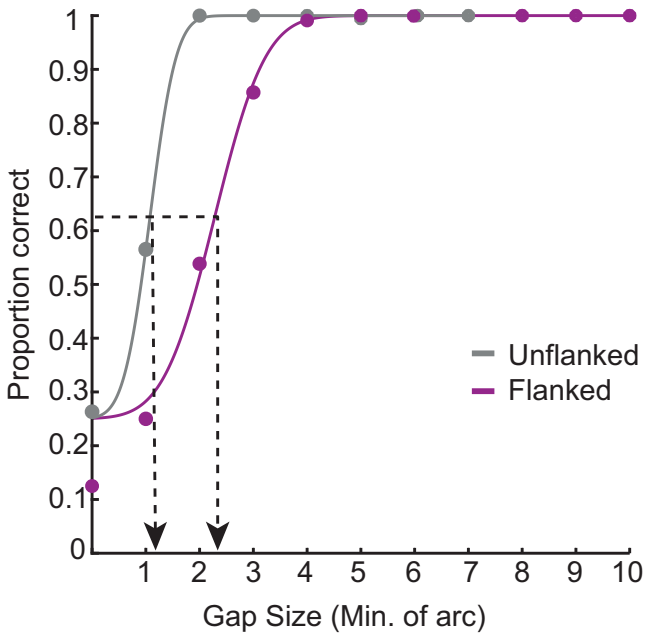

Figure 2. Example responses and psychometric functions for an individual with *CRB1* retinopathy. *Circles* plot the proportion of correct responses at each of the gap sizes presented, separately for the unflanked (*grey*) and flanked (*purple*) conditions. *Solid lines* plot the best-fitting psychometric function for each condition. Gap-size thresholds were taken at 62.5% correct, shown as the *black dashed line* and its corresponding location on the x-axis.

Data Analysis

Behavioral data were collected from the VacMan program and analyzed within MATLAB. Repeated blocks of trials were first combined for each participant from either unflanked or flanked tasks separately, resulting in 70 trials per stimulus condition for all but 2 children in the CRB1 group who completed 35 trials per condition. For each stimulus size that was presented, the corresponding proportion correct scores for responses were then collated. Psychometric functions were fitted to the behavioral data for each stimulus condition using a cumulative Gaussian function with three free parameters (midpoint, slope, and lapse rate). Because the variability added to the QUEST gave variable trial numbers for each gap size, this fitting was performed by weighting the least-squared error value by the number of trials per point. Figure 2 shows an example psychometric function fit to data from a *CRB1* participant, where the grey curve represents the unflanked condition, and the purple curve is the flanked condition. Due to the variability in severity of the disease process in *CRB1* retinopathy, the difference in the unflanked and crowded thresholds was examined, categorized by the disease age of onset, in addition to the group-level analyses. The *CRB1* group was split into two subgroups for this purpose – individuals with a disease onset before the age of 10 years and individuals with an onset when older than 10 years. Paired sample *t*-tests and 2 × 2 mixed-effects ANOVA were performed. Statistical significance was considered if $P < 0.05$. Statistical analysis was performed by MATLAB software (The MathWorks, Ltd., Cambridge, UK).

Results

Participants

A total of 40 individuals were examined: 20 patients with *CRB1*-related retinopathy from 19 unrelated families were included aged between 8 and 52 years old (mean = 26.8 years ± 14.07 years) and 20 age-matched controls (mean age = 26.5 years ± 13.98 years). Within the patients with *CRB1* retinopathy, nine individuals (45%) were pediatric patients (<18 years old). Fourteen (70%) were male patients and six (30%) were female patients. In terms of ethnicity, 17 patients (90%) self-identified as White, 1 as Black (5%), and 1 as southwest Asian (5%). Based on clinical data, retinal imaging, and age of onset, 7 patients were classified as EOSRD/LCA, 3 as CORD, and 10 as MD (Fig. 3). No individuals were clinically classified as resembling RP. Details of demographic characteristics of this cohort are reported in Appendix.

Visual Acuity ETDRS Chart

The mean (± SD) BCVA for patients with *CRB1* retinopathy was 0.55 (± 0.38) logMAR on the ETDRS chart. When examining BCVA by clinical phenotype, the CORD group had the

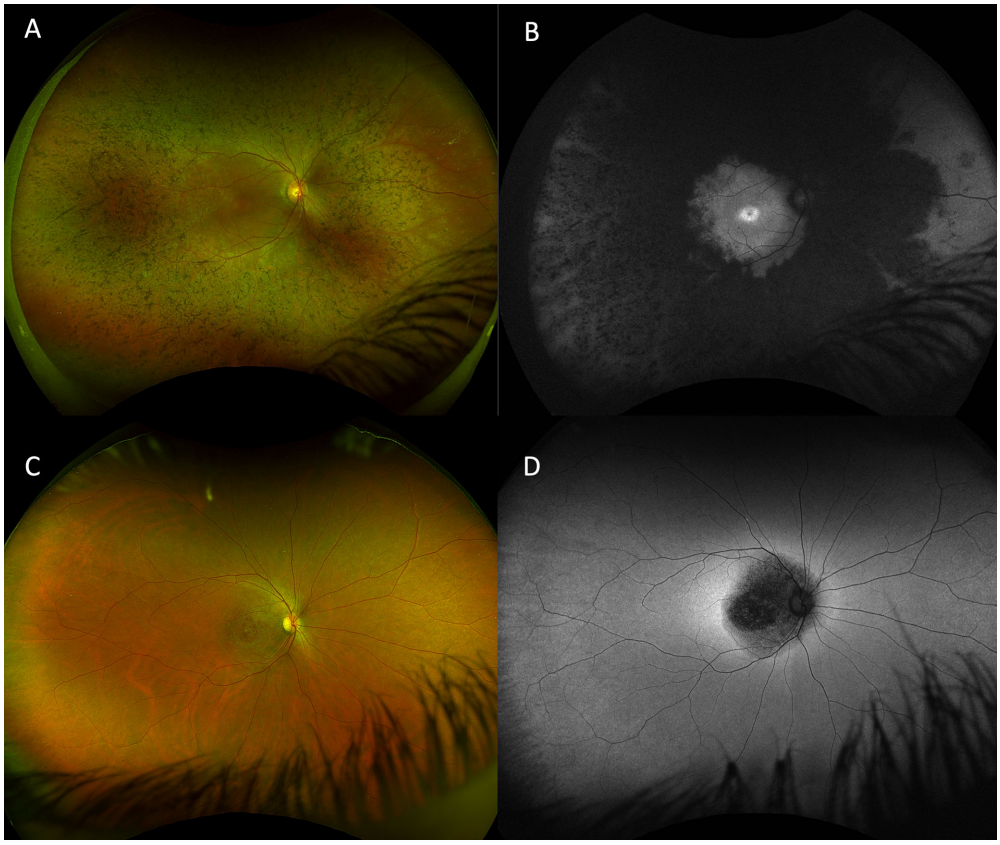

Figure 3. Spectrum of *CRB1* retinopathy phenotypes depicted in widefield color fundus photographs and corresponding fundus autofluorescence (FAF) images. (**A**) Right eye of an 18-year-old male patient with *CRB1*-EOSRD showing peripheral bone spicules and generalized retinal degeneration seen as hypo-autofluorescence (AF) in the FAF image sparing the macular region and a hyper-autofluorescence signal around the fovea (**B**). (**C**) Right eye of a 34-year-old female patient with *CRB1*-MD revealing hypo-AF in the posterior pole with a surrounding hyper-AF ring (**D**).

Investigative Ophthalmology & Visual Science

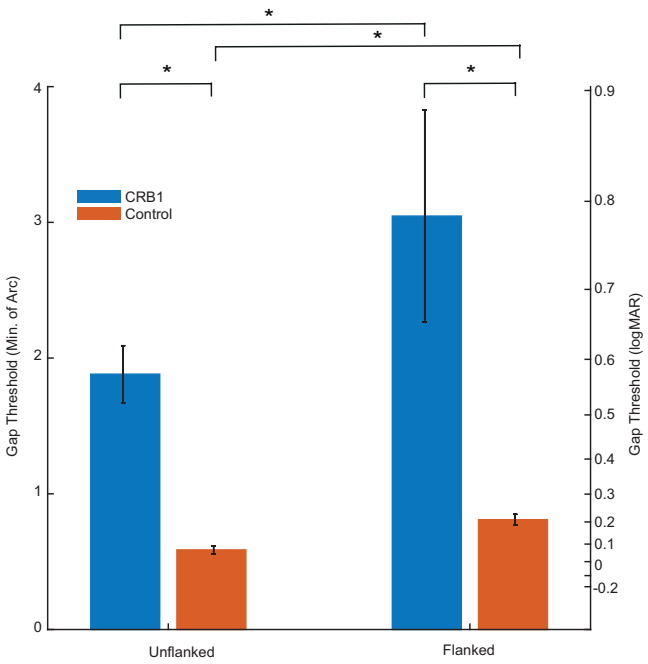

Figure 4. Mean gap-size thresholds for both participant groups, plotted in minutes of arc (left y-axis), with comparison to their logMAR equivalents (right y-axis). The *blue bars* plot thresholds for the *CRB1* group and the *orange bars* plot thresholds for the control group. Error bars represent the SEM, with *asterisks* indicating statistically significantly differences.

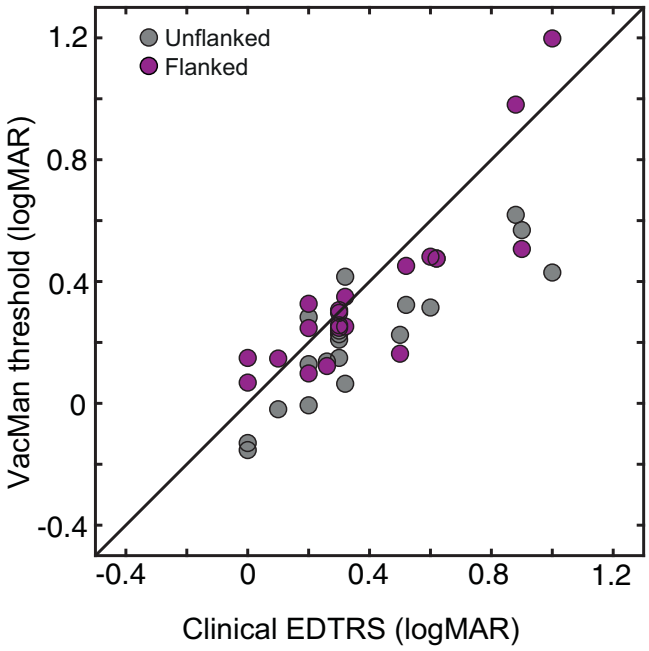

Figure 5. Gap-size thresholds (in logMAR) for *CRB1* individuals for both the unflanked (*grey filled circles*) and the flanked (*purple filled circles*). The y-axis plots VacMan thresholds and the x-axis the clinical ETDRS logMAR values. The *black line* represents perfect correspondence between the two measures.

poorest BCVA with an average of 0.88 (± 0.52) logMAR, followed by the LCA/EOSRD group at 0.57 (± 0.34) logMAR, and the MD group at 0.42 (± 0.34) logMAR. The mean BCVA for control individuals was 0.01 (± 0.03) logMAR on the ETDRS chart. Clinical details are provided in Appendix.

VacMan: Main Results

Gap-size thresholds in the unflanked and flanked conditions are shown for the two participant groups in Figure 4. A 2 × 2 mixed-effects ANOVA revealed a significant main effect of stimulus condition (unflanked versus flanked). This difference is driven by crowding, with both groups exhibiting worse thresholds in the flanked condition compared to the unflanked condition (*CRB1*: $P = 0.006$ and controls: $P < 0.001$). The main effect of participant group (*CRB1* versus controls) was also significant, with patients with *CRB1* retinopathy showing significantly worse thresholds than controls in both unflanked and flanked conditions ($P < 0.001$). The extent of this elevation in crowding was slightly higher in the *CRB1* group than the controls – dividing flanked thresholds by the unflanked baseline reveals that flanked thresholds were 1.65 times higher than unflanked in the *CRB1* group compared to 1.45 in the control group. However, the interaction between participant group and stimulus condition was not significant ($P = 0.904$), suggesting that these elevations in crowding must be considered as broadly in proportion to acuity levels in both groups. Nonetheless, due to the substantially higher unflanked thresholds in the *CRB1* group, the absolute difference in flanked thresholds between the *CRB1* and the control groups was much larger (and, indeed, significantly different, as above), indicating a more disruptive crowding effect in patients with *CRB1* retinopathy. Individuals with *CRB1* gene mutations thus show elevated levels of both acuity and crowding, relative to control participants, although the elevations in crowding are not disproportionately large when compared with their acuity levels.

The unflanked condition of the VacMan task produced lower VA thresholds than the ETDRS test, indicating that participants achieved better visual performance with VacMan. In the flanked condition, the performance of VacMan and ETDRS was similar, as shown by closely aligned thresholds (Fig. 5). Strong correlations between VacMan and ETDRS thresholds were nonetheless observed in both the unflanked ($r = 0.868$, $P < 0.001$) and flanked conditions ($r = 0.748$, $P < 0.001$), demonstrating a close association between the two measures. Figure 5 plots these values against one another, showing that most unflanked thresholds lie below the unity line, whereas crowded data points cluster around it. There is clearly good agreement between the measures.

Age-of-Onset and VacMan

To examine the impact of disease onset on crowding in patients with *CRB1* retinopathy, participants were divided into early onset (before age 10 years) and late onset (after age 10 years) groups (see Fig. 6). A 2 × 2 mixed-effects ANOVA revealed no significant main effect of stimulus condition ($P = 0.582$), but a significant main effect of age-of-onset ($P = 0.007$), indicating that gap-size thresholds differed based on disease onset. There was no significant interaction between onset and crowding condition ($P = 0.504$). Paired sample *t*-tests showed a significant worsening of thresholds in the flanked condition compared to the unflanked condition for the early onset group ($P = 0.007$), but not for the late

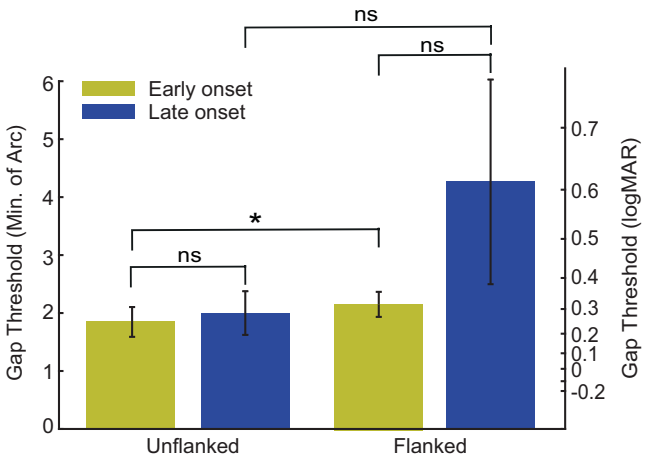

Figure 6. Gap-size thresholds for *CRB1* participants divided by age-of-onset of disease, plotted in minutes of arc (left y-axis), with comparison to their logMAR equivalents (right y-axis). The *green bars* plot thresholds for the early onset *CRB1* group and the *red bar* plots the thresholds for the late onset *CRB1* group. Error bars represent the SEM, with * = significant and ns = not significant.

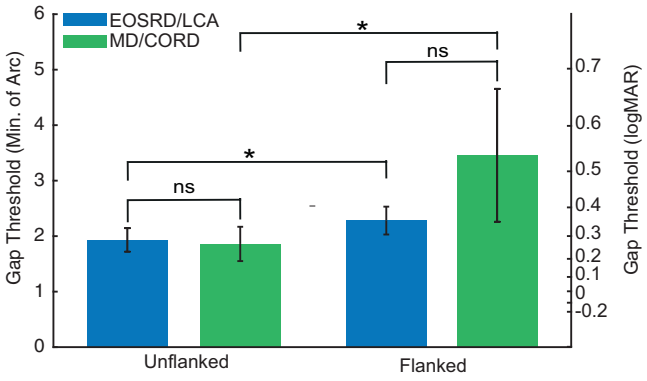

Figure 7. Gap-size thresholds for *CRB1* participants divided by clinical phenotype, plotted in minutes of arc (left y-axis), with comparison to their logMAR equivalents (right y-axis). The *blue bars* plot thresholds for the EOSRD/LCA *CRB1* group and the *green bar* plots the thresholds for the MD/CORD *CRB1* group. Error bars represent the SEM, with * = significant and ns = not significant.

onset group ($P = 0.070$), despite a clear trend in the same direction. Independent samples *t*-tests revealed no significant differences between the early and late onset groups in either the unflanked ($P = 0.964$) or crowded conditions ($P = 0.488$). Thus, although there is some indication that thresholds may be higher in those with a later age of onset, the reduction in sample size for this subgroup analysis reduces our ability to draw clear conclusions.

Next, the impact of the *CRB1* phenotype on thresholds was assessed by dividing participants into EOSRD/LCA (widespread retinal degeneration; $n = 7$) and MD/CORD (macular degeneration; $n = 13$) groups (see Fig. 7). A 2 × 2 mixed-effects ANOVA found no significant main effect of phenotype ($P = 0.608$) but did show a significant main effect of stimulus condition ($P = 0.039$), with elevated thresholds in the flanked condition compared to the unflanked condition. There was no significant interaction between phenotype and crowding ($P = 0.226$). Paired *t*-tests revealed significant increases in thresholds in the flanked condition compared to the unflanked condition for both EOSRD/LCA ($P = 0.033$) and MD/CORD ($P = 0.023$) groups. No significant threshold differences were observed between the EOSRD/LCA and MD/CORD groups in either the unflanked ($P = 0.488$) or flanked conditions ($P = 0.884$). After applying the Bonferroni correction, these differences remained nonsignificant (unflanked: $P = 0.87$ and flanked: $P = 0.955$), despite a trend toward higher thresholds in individuals with MD/CORD (coupled with increased variability).

Next, an enjoyability assessment comparing VacMan and ETDRS was conducted in 17 patients. Among them, 7 were pediatric patients and 10 were adult patients. All pedi-

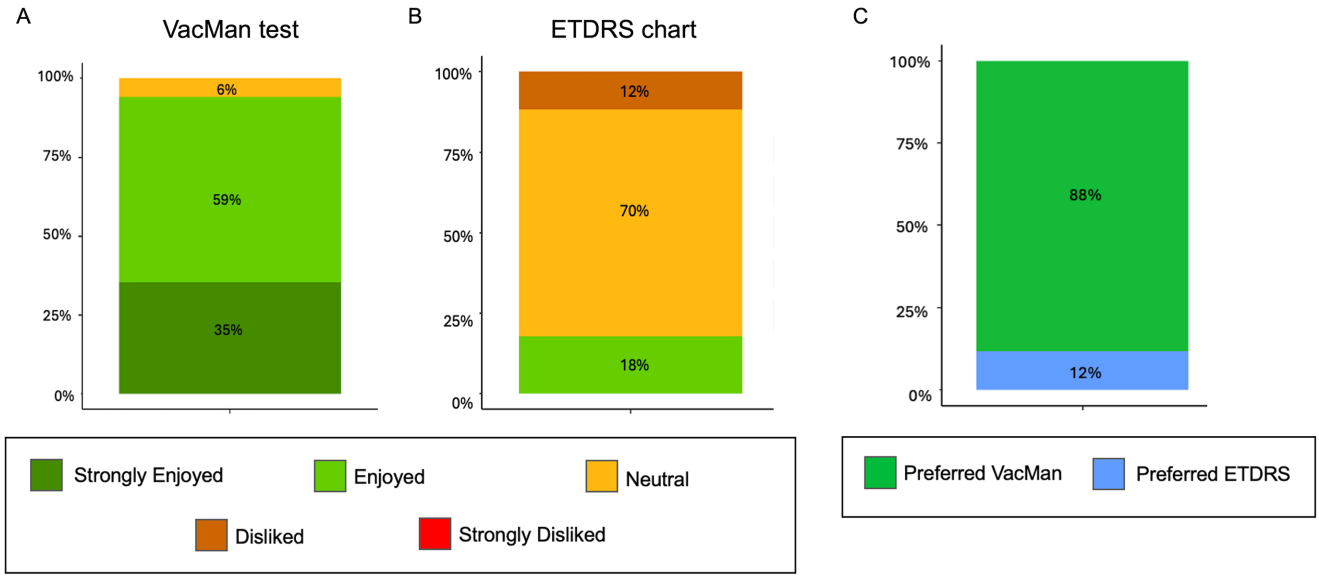

Figure 8. Box plots illustrating the reported enjoyability of the tests. (**A**) Percentage distribution of responses regarding the level of enjoyability when performing the VacMan test. (**B**) Percentage distribution of responses regarding the level of enjoyability when performing the ETDRS chart. (**C**) Preference distribution, with 88% of participants indicating a preference for the VacMan test.

atric patients (100%) reported enjoying or strongly enjoying the test. Among adults, one expressed a neutral response, whereas the remaining nine reported enjoying or strongly enjoying the VacMan test.

In contrast, only 18% of patients reported enjoying the ETDRS test, whereas 70% felt neutral and 12% expressed dislike. When asked about their preference, 88% of the participants indicated a preference for the VacMan test over the ETDRS (see Fig. 8), the remaining 12% who preferred the ETDRS test included one pediatric patient and one adult patient.

Discussion

This study examined VA and crowding in patients with *CRB1* retinopathies compared with aged-matched controls, revealing elevations in *CRB1* retinopathies for acuity thresholds measured with both standard clinical measures (ETDRS) and newer child-friendly measures (VacMan), as well as elevated crowding levels when flankers were added. Our study is the first to demonstrate elevated crowding in individuals with *CRB1* retinopathies compared with controls, in addition to their previously reported elevations in acuity. Although the elevations in crowding were broadly in proportion to acuity levels in both groups (1.65 times above unflanked thresholds in *CRB1* group and 1.45 in the control group), the overall elevation in performance in patients with *CRB1* retinopathy meant that they required larger elements with greater separation between them in order to reach the same performance levels as age-matched controls. These elevations in crowding would exacerbate visual impairments by hindering object recognition in cluttered scenes and may provide a useful outcome metric for treatment programs. All *CRB1* participants successfully completed the VacMan test, and both unflanked and crowded thresholds correlated strongly with the clinical ETDRS test. Individuals with *CRB1* retinopathies also reported the VacMan tests to be more enjoyable than the ETDRS chart.

As treatments for *CRB1* retinopathies continue to advance, the need for new, comprehensive outcome metrics becomes increasingly important.[40–42] Ideally, these metrics should capture various aspects of visual function, detect subtle changes over time, and reduce inherent variability. The current gold standard for assessing visual acuity is the retro-illuminated LogMAR chart, based on the ETDRS optotype.[7] Whereas widely used in clinical settings and trials, and known to correlate with the ellipsoid zone (EZ) integrity on SD-OCT, the ETDRS chart does not fully characterize visual function and may miss subtle changes or variability in visual performance.[9,10] Additionally, discrepancies between VA and structural measures are sometimes observed, especially in certain genotypes like *RDH12* and *CEP290*.[7] Another critical consideration in testing visual function is the adaptability of tests across different age groups, particularly in pediatric populations. The ETDRS chart poses challenges in this context, as preschool children often struggle with letter recognition, and cognitive development differences can complicate acuity measurements.[43] Although modern pediatric charts have been developed following international guidelines, discrepancies remain compared to the ETDRS. For instance, certain picture optotype tests, such as crowded Kay Pictures, tend to overestimate acuity compared with letter tests in both adults and children. However, this discrepancy is not observed with the reference Landolt C test, which forms the basis of the VacMan paradigm.[43]

Our results demonstrate the promise of child-friendly tests, such as the VacMan paradigm, to assess vision similarly to gold-standard measures like the ETDRS, whereas also providing more detailed and reliable information on various aspects of visual function. The VacMan test offers precise, quantitative data derived from psychophysical methods, making it potentially more sensitive to subtle changes in visual function that traditional tests might overlook. In cases where elevations in acuity thresholds are subtle, the additional elevation in flanked thresholds may be more visible using measures such as the VacMan test. Although previous studies on *CRB1* retinopathies have shown relative stability in visual acuity and fields over time,[44] methods like microperimetry, although useful for monitoring residual retinal function, pose challenges, particularly for visually impaired children.[13,44] Notably, visual crowding has not been explored in *CRB1* studies,[4,6,13,15] and there is limited evidence on the use of child-friendly tests as outcome metrics in pediatric populations.[45] This study demonstrated that the VacMan test had a 100% completion rate, and showed elevated crowding in a molecularly confirmed *CRB1* cohort. Thresholds in the unflanked and flanked conditions were also highly correlated with the clinical ETDRS test, although with values that were lower in the unflanked condition relative to the ETDRS. The difference is likely due to the "linear" presentation of the ETDRS charts, including some crowding effects from adjacent letters during testing (14 lines and 5 letters per line),[33] which is further consistent with the agreement between ETDRS values and thresholds in the VacMan flanked condition. The major advantage in the VacMan tests is the clear separation of acuity (measured using isolated elements) and crowding (measured with flanked elements), suggesting that it could be a valuable tool for assessing both acuity and crowding in these patients, particularly in younger populations.

In the course of typical development, elevations in crowding have been shown to persist as late as the age of 12 years old in typical vision,[23,46] unlike acuity which matures to adult levels at around the age of 5 to 6 years old.[47,48] The prolonged development of crowding may explain why elevations in crowding are so common in developmental disorders, such as amblyopia[24,25] and nystagmus[27,28,49]; which have their onset within this period of development. In order to know whether the elevations in crowding with *CRB1* retinopathy varied depending on the age of onset, we divided our patients with *CRB1* into 2 groups based on disease onset: before and after the age of 10 years. Our results in fact showed a trend toward higher thresholds in those with a later age of onset, although individual comparisons were nonsignificant (due to the higher variability and reduced sample sizes for this subgroup analysis). Higher thresholds in the late-onset subgroup may be attributed to the larger proportion of patients with MD/CORD included in this subgroup, conditions that typically involve macular degeneration and thus affecting foveal crowding. In contrast, the early-onset subgroup had a higher number of patients with LCA/EOSRD and, whereas these patients generally experience more severe retinal degeneration, many retain islands of central vision, which could explain their better crowding outcomes. Although there is scant literature of crowding levels in other IRDs, the findings of this study suggest that other IRDs that primarily impact the macular region, such as Stargardt's disease, may also experience higher levels of foveal crowding, similar to those included in this study with MD/CORD. Conversely, IRDs that predomi-

Investigative Ophthalmology & Visual Science

nantly spare the macula, such as RP, might not show the same extent of crowding deficits. Future studies comparing crowding effects in diverse IRD phenotypes would be valuable to confirm the broader applicability of these results and to delineate the influence of macular versus peripheral retinal dysfunction on crowding phenomena.

Understanding visual deficits in patients with pre-existing visual impairment is of paramount importance, particularly in conditions like *CRB1* retinopathies where visual impairments are substantial.[1,4,50] Crowding has been known to occur at a cortical level,[18] potentially operating at multiple levels in the visual hierarchy, modulating activity across cortical regions from V1 to V4.[51–54] Cortical changes in amblyopia[55,56] could similarly drive the elevations in crowding observed in those individuals. Although cortical changes in *CRB1* individuals are unclear, elevated crowding has been reported in patients with glaucoma, who exhibited pronounced visual crowding effects even with mild visual field loss on standard perimetry.[29] Ogata et al. suggested that although crowding is primarily a cortical phenomenon, the loss of retinal ganglion cells in glaucoma may lead to changes and reorganization of cortical receptive fields,[29] a link that was further consolidated by Kwon et al.[57] In the case of patients with *CRB1* gene mutations, the primary loss occurs on the outer retinal layers. This raises important questions about whether elevated crowding in patients with *CRB1* retinopathy is a direct sign of visual impairment or a consequence of retinal degeneration which could potentially be similar to glaucoma, secondary to reorganization of cortical receptive fields. Complicating this picture, visual crowding elevations in our study did not differ significantly across different *CRB1* phenotypes, even though the level of retinal degeneration was heterogenous – the LCA/EOSRD group elicited a widespread retinal degeneration more affected on the periphery, whereas the MD/CORD group had mainly central vision affected and a preserved periphery. Nonetheless, the link between retinal degeneration and cortical changes in these conditions is a topic warranting further research.

In the real world, crowding elevations can compromise reading ability,[58] object recognition[59] visual search,[60] and driving,[61] impacting daily tasks and mobility. The elevations in flanked thresholds found for individuals with *CRB1* retinopathies would similarly be likely to hinder these abilities. Strategies such as increasing spacing between objects or using assistive devices may help mitigate the effects of visual crowding in individuals with macular disease forced to rely on their peripheral vision.[62] One such approach is Word Mode, a peripheral reading protocol that reduces crowding by presenting each word in isolation but in a position that mimics its natural position in the line of text being read, with each new word elicited using a self-paced button press proposing that the level of reading efficiency may return reading as a viable activity to many individuals with macular disease.[63] Other approaches, such as enhanced text spacing and interline spacing,[62,64] could be further advised in patients who still have good vision but struggle with daily tasks. Nonetheless, there is still a need to understand visual deficits and subsequently, vision-related quality of life in patients with IRDs to provide further support. Interestingly, Karuntu et al., in their 4-year longitudinal study, observed a decline in vision-related quality of life questionnaires in patients with *CRB1* retinopathy using National Eye Institute Visual Function Questionnaire 25 (NEI-VFQ-25). This decline was particularly pronounced in the "near activities" domain, raising the question of whether increased visual crowding contributes to this impairment. Additionally, the "socio-emotional" domain was substantially affected, with changes correlating to a decline in macular sensitivity as measured by microperimetry.[65] Future research should focus on longitudinal studies to evaluate how visual function and crowding in patients with *CRB1* evolve over time. A prospective 2-year deep phenotyping study of patients with *CRB1* retinopathies at Moorfields Eye Hospital is now underway and baseline measurements, including the VacMan test, have been completed with patient-reported outcome measures (PROMs) now incorporated. This prospective study will explore whether the VacMan test can more accurately detect changes in vision over time compared to the ETDRS chart, and whether visual crowding changes with disease progression. Additional investigation into the applicability of the VacMan test across other inherited retinal diseases could provide valuable insights into its broader utility and potentially integrating into clinical trials as a child-friendly outcome metric.

Limitations

Several limitations to the study are worth highlighting. First, *CRB1* retinopathies represent a rare subset of the IRDs population, and although this study is among the largest case series for this rare group, the sample size remains small, with limitations in statistical power and sample heterogeneity. This may impact upon the reliability of the analyses regarding our thresholds, most notably with our subgroup analyses split by age-of-onset and phenotype, and the reader should, of course, treat these results with appropriate caution. Further studies with bigger sample size are recommended to enhance the statistical power and external validity of the findings. Test reliability (test-retest repeatability) was not assessed in this study, although our longitudinal investigations will provide some insight into this. Finally, our testing was conducted binocularly, unlike in cases like amblyopia where monocular testing is the norm. Although IRDs tend to be symmetrical in disrupting both eyes, there is a certain level of asymmetry noted. It may be ideal in future work to perform both tests unilaterally to assess disease progression.

Conclusions

This study explores the use of the child-friendly VacMan test and compares it to the reference standard ETDRS chart. In addition to deficits in acuity, we demonstrate that visual crowding effects are elevated in individuals with *CRB1*-related retinopathies. Assessing visual crowding separately from acuity, using the VacMan paradigm, provides valuable insights into the functional visual deficits associated with *CRB1*. These measures nonetheless showed strong correlations with the clinical ETDRS test, as well as being broadly accessible – all patients with *CRB1* retinopathies successfully completed the VacMan test. These findings have significant implications for understanding the impact of crowding on daily tasks for patients with *CRB1* retinopathies and underscore the potential of child-friendly computerized visual tests for IRDs.

Acknowledgments

The authors thank to Trust 205174/Z/16/Z, Fight for Sight, Moorfields Eye Charity and the NIHR Biomedical Research Centre at Moorfields Eye Hospital NHS Trust and UCL Institute of Ophthalmology.

Investigative Ophthalmology & Visual Science

The sponsor and funding organisation had no role in the design or conduct of this research.

Disclosure: **A.C. Rodriguez-Martinez**, None; **V.K. Tailor-Hamblin**, None; **B.E. Higgins**, None; **P.R. Jones**, None; **T.M. Dekker**, None; **R.H. Henderson**, None; **J.A. Greenwood**, None; **M. Moosajee**, None

References

1. Rodriguez-Martinez AC, Higgins BE, Tailor-Hamblin V, et al. Foveal hypoplasia in CRB1-related retinopathies. *Int J Mol Sci*. 2023;24(18):13932.
2. Stehle IF, Imventarza JA, Woerz F, et al. Human CRB1 and CRB2 form homo- and heteromeric protein complexes in the retina. *Life Sci Alliance*. 2024;7(6):e202302440.
3. Boon N, Wijnholds J, Pellissier LP. Research models and gene augmentation therapy for CRB1 retinal dystrophies. *Front Neurosci*. 2020;14:860.
4. Varela MD. CRB1-associated retinal dystrophies: genetics, clinical characteristics, and natural history. *Am J Ophthalmol*. 2023;246:107–121.
5. Henderson RH, Mackay DS, Li Z, et al. Phenotypic variability in patients with retinal dystrophies due to mutations in CRB1. *Br J Ophthalmol*. 2011;95(6):811–817.
6. Nguyen X-T-A, Talib M, van Schooneveld MJ, et al. A two-year prospective natural history study in patients with CRB1-associated retinal dystrophies: establishing clinical endpoints for future gene therapy trials. *Invest Ophthalmol Vis Sci*. 2020;61:3051.
7. Daich Varela M, Georgiou M, Hashem SA, Weleber RG, Michaelides M. Functional evaluation in inherited retinal disease. *Br J Ophthalmol*. 2022;106(11):1479–1487.
8. Beck RW, Maguire MG, Bressler NM, Glassman AR, Lindblad AS, Ferris FL. Visual acuity as an outcome measure in clinical trials of retinal diseases. *Ophthalmology*. 2007;114(10):1804–1809.
9. Vingopoulos F, Wai KM, Katz R, Vavvas DG, Kim LA, Miller JB. Measuring the contrast sensitivity function in non-neovascular and neovascular age-related macular degeneration: the quantitative contrast sensitivity function test. *J Clin Med*. 2021;10(13):2768.
10. Yu HJ, Kaiser PK, Zamora D, et al. Visual acuity variability: comparing discrepancies between Snellen and ETDRS measurements among subjects entering prospective trials. *Ophthalmol Retina*. 2021;5(3):224–233.
11. Xiong YZ, Kwon M, Bittner AK, Virgili G, Giacomelli G, Legge GE. Relationship between acuity and contrast sensitivity: differences due to eye disease. *Invest Ophthalmol Vis Sci*. 2020;61(6):40.
12. Elfadaly D, Abdelrazik ST, Thomas PBM, Dekker TM, Dahlmann-Noor A, Jones PR. Can psychophysics be fun? Exploring the feasibility of a gamified contrast sensitivity function measure in amblyopic children aged 4-9 years. *Front Med (Lausanne)*. 2020;7:469.
13. Roshandel D, Thompson JA, Heath Jeffery RC, et al. Multimodal retinal imaging and microperimetry reveal a novel phenotype and potential trial end points in CRB1-associated retinopathies. *Transl Vis Sci Technol*. 2021;10(2):38.
14. Roshandel D, Monitoring disease progression in retinitis pigmentosa [degree of Doctor of Philosophy thesis]. The University of Western Australia; Faculty of Healthy and Medical Sciences Centre for Ophthalmology and Visual Science Lions Eye Institute: 2022. Available at: https://api.research-repository.uwa.edu.au/ws/files/192360469/THESIS_DOCTOR_OF_PHILOSOPHY_ROSHANDEL_Danial_2022.pdf.
15. Talib M, Van Cauwenbergh C, De Zaeytijd J, et al. CRB1-associated retinal dystrophies in a Belgian cohort: genetic characteristics and long-term clinical follow-up. *Br J Ophthalmol*. 2022;106(5):696–704.
16. Csaky K, Ferris F, 3rd, Chew EY, Nair P, Cheetham JK, Duncan JL. Report From the NEI/FDA Endpoints Workshop on Age-Related Macular Degeneration and Inherited Retinal Diseases. *Invest Ophthalmol Vis Sci*. 2017;58(9):3456–3463.
17. Whitney D, Levi D. Visual crowding: a fundamental limit on conscious perception and object recognition. *Trends Cogn Sci*. 2011;15(4):160–168.
18. Flom MC, Heath GG, Takahashi E. Contour interaction and visual resolution: contralateral effects. *Science*. 1963;142(3594):979–980.
19. Bouma H. Interaction effects in parafoveal letter recognition. *Nature*. 1970;226(5241):177–178.
20. Toet A, Levi DM. The two-dimensional shape of spatial interaction zones in the parafovea. *Vision Res*. 1992;32(7):1349–1357.
21. Pelli DG, Palomares M, Majaj NJ. Crowding is unlike ordinary masking: distinguishing feature integration from detection. *J Vis*. 2004;4(12):1136–1169.
22. Jeon ST, Hamid J, Maurer D, Lewis TL. Developmental changes during childhood in single-letter acuity and its crowding by surrounding contours. *J Exp Child Psychol*. 2010;107(4):423–437.
23. Atkinson J, Anker S, Evans C, Hall R, Pimm-Smith E. Visual acuity testing of young children with the Cambridge Crowding Cards at 3 and 6 m. *Acta Ophthalmol (Copenh)*. 1988;66(5):505–508.
24. Levi DM, Klein SA. Vernier acuity, crowding and amblyopia. *Vision Res*. 1985;25(7):979–991.
25. Greenwood JA, Tailor VK, Sloper JJ, Simmers AJ, Bex PJ, Dakin SC. Visual acuity, crowding, and stereo-vision are linked in children with and without amblyopia. *Invest Ophthalmol Vis Sci*. 2012;53(12):7655–7665.
26. Chung ST, Bedell HE. Effect of retinal image motion on visual acuity and contour interaction in congenital nystagmus. *Vision Res*. 1995;35(21):3071–3082.
27. Pascal E, Abadi RV. Contour interaction in the presence of congenital nystagmus. *Vision Res*. 1995;35(12):1785–1789.
28. Tailor V, Theodorou M, Dahlmann-Noor AH, Dekker TM, Greenwood JA. Eye movements elevate crowding in idiopathic infantile nystagmus syndrome. *J Vis*. 2021;21(13):9.
29. Ogata NG, Boer ER, Daga FB, Jammal AA, Stringham JM, Medeiros FA. Visual crowding in glaucoma. *Invest Ophthalmol Vis Sci*. 2019;60(2):538–543.
30. Shamsi F, Liu R, Kwon M. Binocularly asymmetric crowding in glaucoma and a lack of binocular summation in crowding. *Invest Ophthalmol Vis Sci*. 2022;63(1):36.
31. Tanriverdi D, Al-Nosairy KO, Hoffmann MB, Cornelissen FW. Assessing visual crowding in participants with preperimetric glaucoma using eye movement and manual response paradigms. *Transl Vis Sci Technol*. 2024;13(9):8.
32. Lalor SJH, Formankiewicz MA, Waugh SJ. Crowding and visual acuity measured in adults using paediatric test letters, pictures and symbols. *Vision Res*. 2016;121:31–38.
33. Song S, Levi DM, Pelli DG. A double dissociation of the acuity and crowding limits to letter identification, and the promise of improved visual screening. *J Vis*. 2014;14(5):3.
34. Kalpadakis-Smith AV, Tailor VK, Dahlmann-Noor AH, Greenwood JA. Crowding changes appearance systematically in peripheral, amblyopic, and developing vision. *J Vis*. 2022;22(6):3.
35. Brainard D. The Psychophysics Toolbox. *Spat Vis*. 1997;10(4):433–436.

36. Pelli D. The VideoToolbox software for visual psychophysics: transforming numbers into movies. *Spat Vis*. 1997;10(4):437–442.
37. Sloan LL. New test charts for the measurement of visual acuity at far and near distances. *Am J Ophthalmol*. 1959;48:807–813.
38. Watson A, Pelli D. QUEST: a Bayesian adaptive psychometric method. *Percept Psychophys*. 1983;33(2):113–120.
39. Manning C, Jones PR, Dekker TM, Pellicano E. Psychophysics with children: investigating the effects of attentional lapses on threshold estimates. *Atten Percept Psychophys*. 2018;80(5):1311–1324.
40. Boon N, Lu X, Andriessen CA, et al. AAV-mediated gene augmentation therapy of CRB1 patient-derived retinal organoids restores the histological and transcriptional retinal phenotype. *Stem Cell Reports*. 2023;18(5):1123–1137.
41. Buck TM, Vos RM, Alves CH, Wijnholds J. AAV-CRB2 protects against vision loss in an inducible CRB1 retinitis pigmentosa mouse model. *Mol Ther Methods Clin Dev*. 2021;20:423–441.
42. Alves CH, Wijnholds J. AAV-mediated gene therapy for CRB1-hereditary retinopathies. In: *In Vivo and Ex Vivo Gene Therapy for Inherited and Non-Inherited Disorders*. 2018; Intechopen. Available from: http://dx.doi.org/10.5772/intechopen.79308.
43. Anstice NS, Jacobs RJ, Simkin SK, Thomson M, Thompson B, Collins AV. Do picture-based charts overestimate visual acuity? Comparison of Kay Pictures, Lea Symbols, HOTV and Keeler logMAR charts with Sloan letters in adults and children. *PLoS One*. 2017;12(2):e0170839.
44. Nguyen XT, Talib M, van Schooneveld MJ, et al. CRB1-associated retinal dystrophies: a prospective natural history study in anticipation of future clinical trials. *Am J Ophthalmol*. 2022;234:37–48.
45. Crossland MD, Dekker TM, Dahlmann-Noor A, Jones PR. Can children measure their own vision? A comparison of three new contrast sensitivity tests. *Ophthalmic Physiol Opt*. 2024;44:5–16.
46. Jeon S, Hamid J, Maurer D, Lewis TL. Developmental changes during childhood in single-letter acuity and its crowding by surrounding contours. *J Exp Child Psychol*. 2010;107(4):423–437.
47. Simons K. Visual acuity norms in young children. *Surv Ophthalmol*. 1983;28(2):84–92.
48. Leat SJ, Yadav NK, Irving EL. Development of visual acuity and contrast sensitivity in children. *J Optom*. 2009;2(1):19–26.
49. Chung S. Size or spacing: which limits letter recognition in people with age-related macular degeneration? *Vis Res*. 2014;101:167–176.
50. Talib M, van Schooneveld MJ, Wijnholds J, et al. Defining inclusion criteria and endpoints for clinical trials: a prospective cross-sectional study in CRB1-associated retinal dystrophies. *Acta Ophthalmol*. 2021;99(3):e402–e414.
51. Motter BC, Simoni DA. The roles of cortical image separation and size in active visual search performance. *J Vis*. 2007;7(2):6.1–6.15.
52. Anderson EJ, Dakin SC, Schwarzkopf DS, Rees G, Greenwood JA. The neural correlates of crowding-induced changes in appearance. *Curr Biol*. 2012;22(13):1199–1206.
53. He D, Wang Y, Fang F. The critical role of V2 population receptive fields in visual orientation crowding. *Curr Biol*. 2019;29(13):2229–2236.e3.
54. Henry CA, Kohn A. Feature representation under crowding in macaque V1 and V4 neuronal populations. *Curr Biol*. 2022;32(23):5126–5137.e3.
55. Kiorpes L, McKee SP. Neural mechanisms underlying amblyopia. *Curr Opin Neurobiol*. 1999; 9(4):480–486.
56. Clavagnier S, Dumoulin SO, Hess RF. Is the cortical deficit in amblyopia due to reduced cortical magnification, loss of neural resolution, or neural disorganization? *J Neurosci*. 2015;35(44):14740–14755.
57. Kwon M, Liu R. Linkage between retinal ganglion cell density and the nonuniform spatial integration across the visual field. *Proc Natl Acad Sci USA*. 2019;116(9):3827–3836.
58. Falkenberg H, Rubin G, Bex P. Acuity, crowding, reading and fixation stability. *Vis Res*. 2007;47(1):126–135.
59. Pelli DG, Tillman KA. The uncrowded window of object recognition. *Nat Neurosci*. 2008;11(10):1129–1135.
60. Gheri C, Morgan MJ, Solomon JA. The relationship between search efficiency and crowding. *Perception*. 2007;36(12):1779–1787.
61. Xia Y, Manassi M, Nakayama K, Zipser K, Whitney D. Visual crowding in driving. *J Vis*. 2020;20(6):1.
62. Blackmore-Wright S, Georgeson MA, Anderson SJ. Enhanced text spacing improves reading performance in individuals with macular disease. *PLoS One*. 2013;8(11):e80325.
63. Wallis S, Yang Y, Anderson SJ. Word Mode: a crowding-free reading protocol for individuals with macular disease. *Sci Rep*. 2018;8(1):1241.
64. Calabrèse A, Bernard JB, Hoffart L, et al. Small effect of interline spacing on maximal reading speed in low-vision patients with central field loss irrespective of scotoma size. *Invest Ophthalmol Vis Sci*. 2010;51(2):1247–1254.
65. Karuntu JS, Nguyen XTA, Talib M, et al. Quality of life in patients with CRB1-associated retinal dystrophies: a longitudinal study. *Acta Ophthalmol*. 2024;102(4):469–477.

Investigative Ophthalmology & Visual Science

Appendix

Table A1. Summary of subject demographics, genetic results, and clinical characteristics of the 20 patients with biallelic pathogenic variants in the *CRB1* gene

Family Number	Subject	Gender	Ethnicity	Age	Phenotype	Zygosity	Variant 1 cDNA Variant 1 Protein	Variant 2 cDNA Variant 2 Protein
45590	01	F	Black African	29	MD	Homozygous	c.2506C>A p.Pro836Thr	
46120	02	F	White	17	EOSRD/LCA	Heterozygous	c.455G>A p.Cys152Tyr	c.3014A>T p.Asp1005Val
35083	03	M	White	39	MD	Heterozygous	c.498_506del p.Ile167_Gly169del	c.4142C>G p.Pro1381Arg
43560	04	F	White	48	MD	Heterozygous	c.498_506del p.Ile167_Gly169del	c.1696G>T p.Glu556Ter
38236	05	M	White	47	MD	Heterozygous	c.498_506del p.Ile167_Gly169del	c.584G>T p.Cys195Phe
38229	06	M	White	24	EOSRD/LCA	Heterozygous	c.2129A>T p.Glu710Val	c.3988del p.Glu1330Serfs*11
Z889804	07	M	Asian	13	CORD	Heterozygous	c.498_506del p.Ile167_Gly169del	c.4005+1G>A N/A
	08	M	White	15	MD	Heterozygous	c.498_506del p.Ile167_Gly169del	c.1576C>T p.Arg525*
42270	09	M	White	52	MD	Heterozygous	c.498_506del p.Ile167_Gly169del	c.2401A>T p.Lys801*
31953	10	F	White	16	EOSRD/LCA	Heterozygous	c.2548G>A p.Gly850Ser	c.4006-10A>G N/A
37161	11	M	White	17	MD	Heterozygous	c.498_506del p.Ile167_Gly169del	c.2308G>T p.Gly770Cys
46830	12	M	White	10	EOSRD/LCA	Heterozygous	c.2843G>A p.Cys948Tyr	c.1712A>C p.Glu571Ala
44092	13	F	White	11	MD	Heterozygous	c.498_506del p.Ile167_Gly169del	c.2843G>A p.Cys948Tyr
35283	14	M	White	11	EOSRD/LCA	Homozygous	c.2843G>A p.Cys948Tyr	
35283	15	M	White	8	EOSRD/LCA	Homozygous	c.2843G>A p.Cys948Tyr	
32038	16	M	White	40	CORD	Heterozygous	c.498_506del p.Ile167_Gly169del	c.1431delG p.Ser478Profs*24
33707	17	M	White	29	MD	Heterozygous	c.498_506del p.Ile167_Gly169del	c.3827_3828del p.Glu1276Valfs*4
47941	18	M	White	18	EOSRD/LCA	Homozygous	c.2291G>A p.Arg764His	
21819	19	M	White	33	CORD	Homozygous	c.470G>C p.Cys157Ser	c.2506C>A p.Pro836Thr
35229	20	F	White	34	MD	Heterozygous	c.498_506del p.Ile167_Gly169del	c.2290C>T p.Arg764Cys

CORD, cone-rod dystrophy; EOSRD, early onset severe retinal dystrophy; LCA, Leber congenital amaurosis; MD, macular dystrophy.

Investigative Ophthalmology & Visual Science